

**Design of 2D/1D Bi<sub>2</sub>MoO<sub>6</sub>/Bi<sub>19</sub>S<sub>27</sub>Br<sub>3</sub> direct Z-scheme heterojunction with  
built-in internal electric field for enhanced CO<sub>2</sub> photocatalytic reduction  
performance**

Zakaria Ismail<sup>a</sup>, You Li<sup>a</sup>, Jian Lei<sup>b</sup>, Saira Man<sup>a</sup>, Khadija Tul Kubra<sup>c</sup>, Chao Zhang<sup>b\*</sup>, Jingxiang  
Low<sup>d</sup>, Yujie Xiong<sup>a,b\*</sup>

*<sup>a</sup>School of Chemistry and Materials Science, Hefei National Research Center for Physical Sciences at the Microscale, Key Laboratory of Precision and Intelligent Chemistry, University of Science and Technology of China, Hefei, Anhui 230026, China*

*<sup>b</sup>Anhui Engineering Research Center of Carbon Neutrality, The Key Laboratory of Functional Molecular Solids, Ministry of Education, Anhui Laboratory of Molecular-Based Materials, College of Chemistry and Materials Science, Anhui Normal University, Wuhu, Anhui 241002, China*

*<sup>c</sup>National Synchrotron Radiation Laboratory, School of Nuclear Science and Technology, The Experimental Center of Engineering and Material Sciences, University of Science and Technology of China, Hefei, Anhui 230026 China.*

*<sup>d</sup>School of Physical Science and Technology, School of Materials Science and Engineering, Tiangong University, Tianjin 300387, China*

*E-mail: yjxiong@ustc.edu.cn; zc1992@ustc.edu.cn*

## **Experimental section**

### **Characterizations**

The phase characterization of the prepared photocatalyst was investigated by powder X-ray diffractometer by using Philips X'pert X-ray diffraction system with Cu  $K\alpha$  radiation ( $\lambda=0.15419$  nm) in the range of  $10^\circ$ – $80^\circ$  with a scanning rate of  $5^\circ \text{ min}^{-1}$ . Fourier-transformed infrared spectra were obtained using a Nicolet 6700 FTIR spectrometer (USA). The infrared thermograms were taken via a thermos imager (Hikvision H10, China). The morphologies of the prepared samples were investigated by using scanning electron microscopy (SEM, Zeiss Supra 40 field-emission scanning electron microscope) at accelerating voltage of 1-30 kV. Transmission electron microscopy (TEM) and high-resolution TEM (HRTEM) images, and energy-dispersive X-ray spectroscopy (EDS) mapping profiles, were recorded on a Talos F200X field-emission high-resolution transmission electron microscope at 200 kV. The surface electronic states of the samples were recorded via X-ray photoelectron spectroscopy by using a Thermo ESCALAB 250 Xi spectrometer with an excitation source of monochromatic Al- $K\alpha$  X-ray ( $h\nu=1486.6$ ) and pass energy of 40 eV. The values of binding energies were calibrated with the C 1s peak at 284.8 eV of the surface adventitious carbon. UV-visible diffuse reflectance (DRS) data were recorded in the spectral region of 200-1200 nm by using Shimadzu solid spec-3700 spectrophotometer. Steady-state photoluminescence (PL) spectra were recorded on Edinburgh FL21000 (Horiba Scientific) with an excitation wavelength of 325 nm. The isotopic composition of carbon was determined by gas chromatography-mass spectrometry (GC-MS Agilent 7890A-5975) using helium as the carrier gas. The  $\text{N}_2$  absorption-desorption isotherms and Brunauer-Emmett-Telle (BET) surface area measurements were obtained with Micromeritics ASAP2020 instrument. The sample was degassed at 393 K for 5 h and then analyzed at 77 K to determine the surface area and porosity.

### **$\text{CO}_2$ photocatalytic reduction test**

The  $\text{CO}_2$  photocatalytic reduction process was conducted at room temperature. Normally, 3 mg photocatalyst was dispersed into 6 mL DI water in 35 mL quartz reactor tube, high purity  $\text{CO}_2$  (99.99%) was pumped into the reactor for 15 min with a fixed flow. Then the reactor was tightly sealed. Then the light irradiation was turned on to drive the reaction system a 300 W Xenon lamp (Perfect light PLS-SXE300,  $\geq 400$  nm) with a light intensity of  $300 \text{ mW/cm}^2$ . The gaseous

products were quantified by a gas chromatograph (GC, Agilent GC 7890A, polymer pellet molecular sieve) equipped with a thermal conductivity detector (TCD) and flame ionization detector (FID), for testing, 2 mL of gas was collected using a syringe from the reactor and injected into the GC for quantitative analysis.

### **Electrochemical measurements**

The photoelectrochemical tests were conducted using a three-electrode system (CHI-660E). Mixed solution, Pt electrode and Ag/AgCl electrode were used as electrolyte, auxiliary electrode and reference electrode respectively. The solution was prepared by 0.5 M Na<sub>2</sub>SO<sub>4</sub>. 3 mg of sample was added to the mixed solution (0.5 mL ethanol and 20 μL Nafion solution) and sonicated for 30 min. Then 30 μL mixed solution was dropped on fluorine-doped tin oxide (FTO, 1 × 2 cm<sup>2</sup>) as working electrode.

### **EPR with DMPO trapping test**

Electron paramagnetic resonance (EPR) measurements using 5,5-dimethyl-1-pyrroline-N-oxide (DMPO) as a spin-trapping agent were performed on a Bruker ESP 300E spectrometer. To detect <sup>•</sup>OH radicals, a sample was prepared by dispersing 5 mg of catalyst in 1 mL of DI, followed by the addition of 8 μL of DMPO. For the detection of superoxide <sup>•</sup>O<sub>2</sub><sup>-</sup> radicals, DI water was replaced with methanol. The radical formation was assessed by comparing EPR signals obtained under dark conditions and under light irradiation.

### **In situ DRIFTS measurements**

In situ DRIFTS measurements were performed using a Bruker IFS 66V Fourier- transform spectrometer (equipped with a Harrick diffuse reflectance accessory at the infrared spectroscopy and Micro spectroscopy end station (BL01B) NSRL). Each spectrum was recorded by averaging 256 scans at resolution of 4 cm<sup>-1</sup>. The samples were placed in an infrared (IR) chamber sealed with Zinc Selenide (ZnSe) windows, which are specifically designed to examine highly scattered powder samples in diffuse reflection mode. After sample loading, the chamber was purged with argon gas (99.99%) for 30 min. Then, the spectrum was collected as background spectrum. During the in-situ characterization CO<sub>2</sub> (99.99%) was continuously introduced into the chamber and the 300 W Xe lamp was used as light source for in-situ DRIFT characterization.

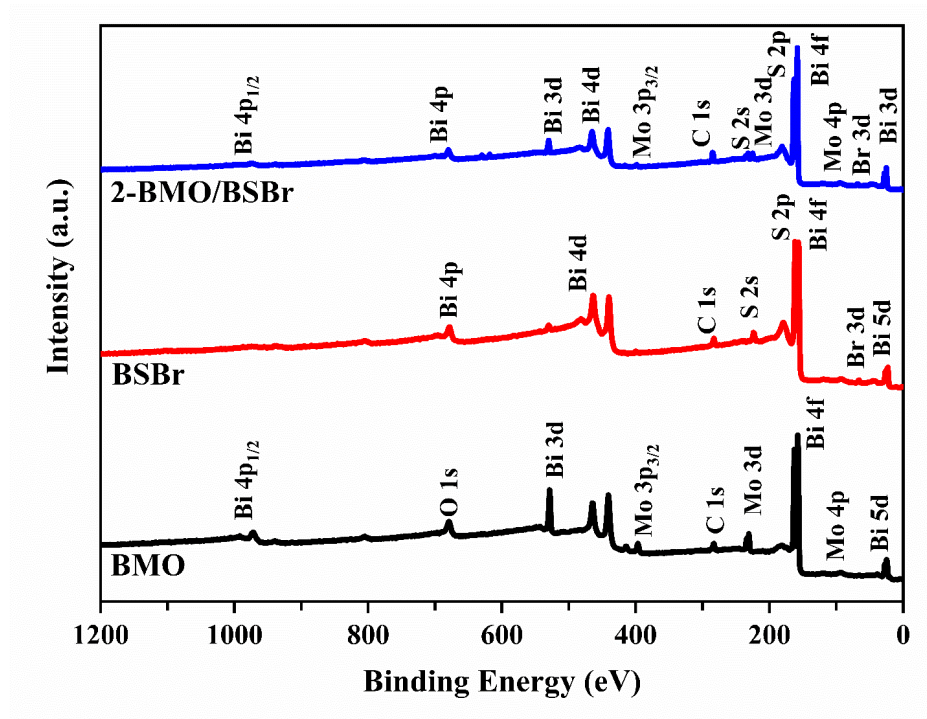


**Figure S1.** High resolution XPS survey spectra of BMO, BSBr, and 2-BMO/BSBr.

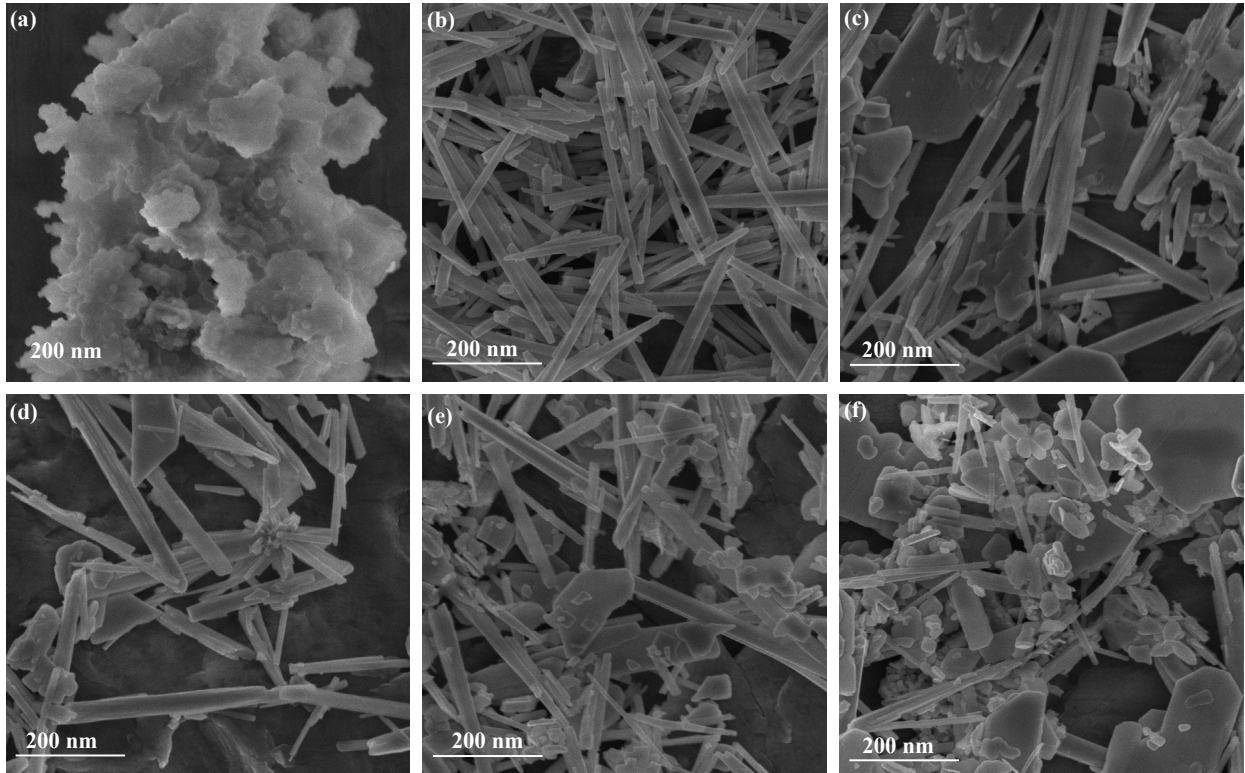


**Figure S2.** SEM images of a) BMO, b)BSBr, c)1-BMO/BSB d), 2-BMO/BSB, e)3-BMO/BSB, and f)4-BMO/BSB samples.

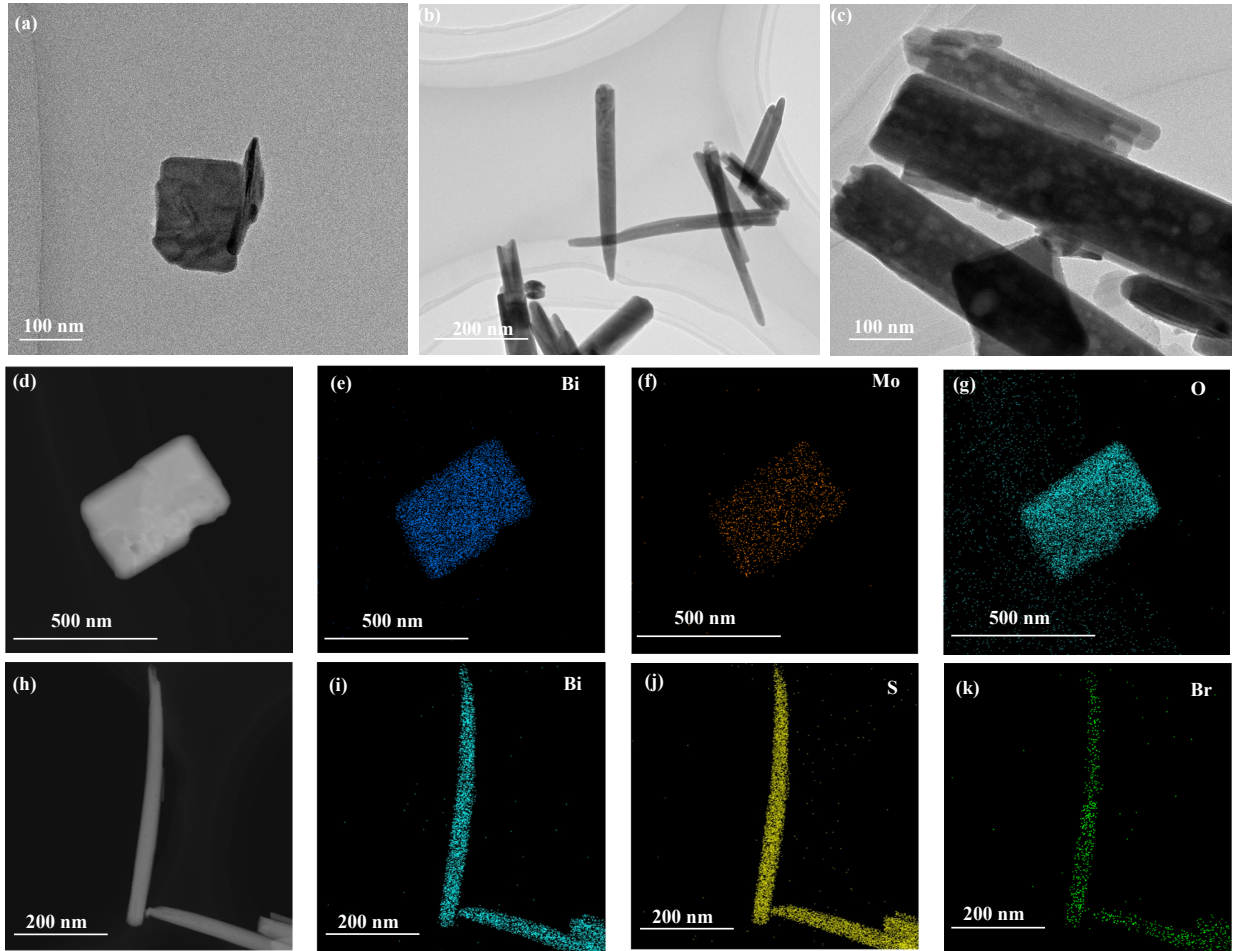


**Figure S3.** a-c) TEM images of BMO (a), BSBr (b), and 2-BMO/BSBr (c) samples. d-k) EDS element mapping of BMO and BSBr samples.

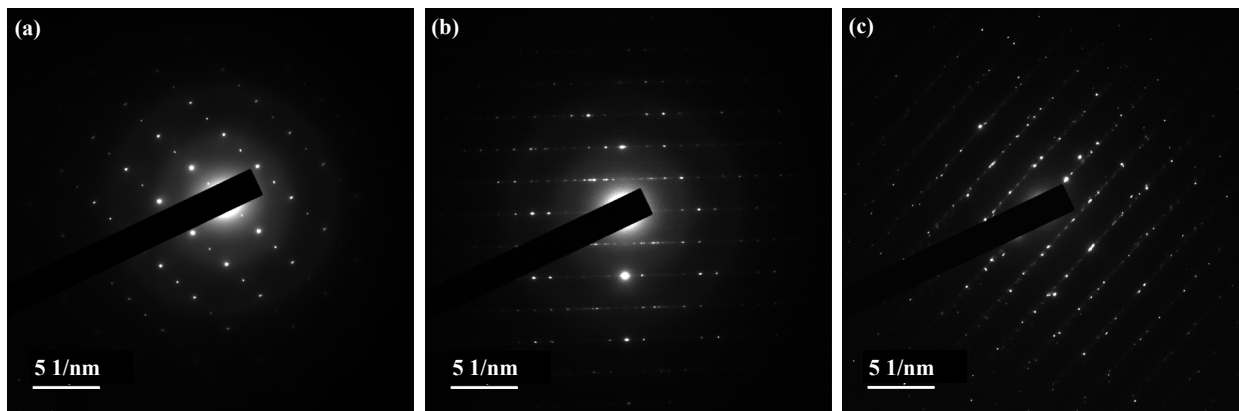


Figure S4. a-c) SEAD patterns of BMO, BSBBr, and 2-BMO/BSBr samples.

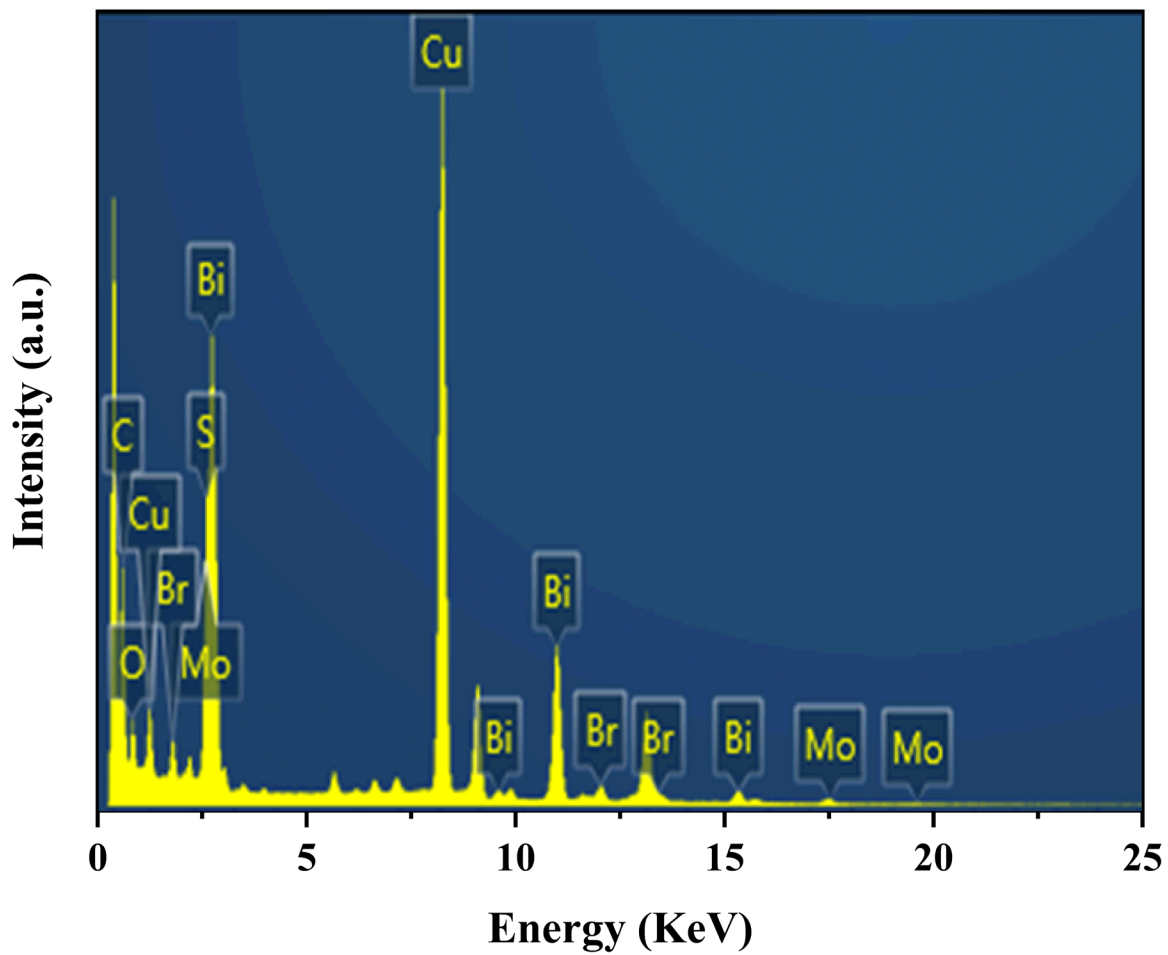
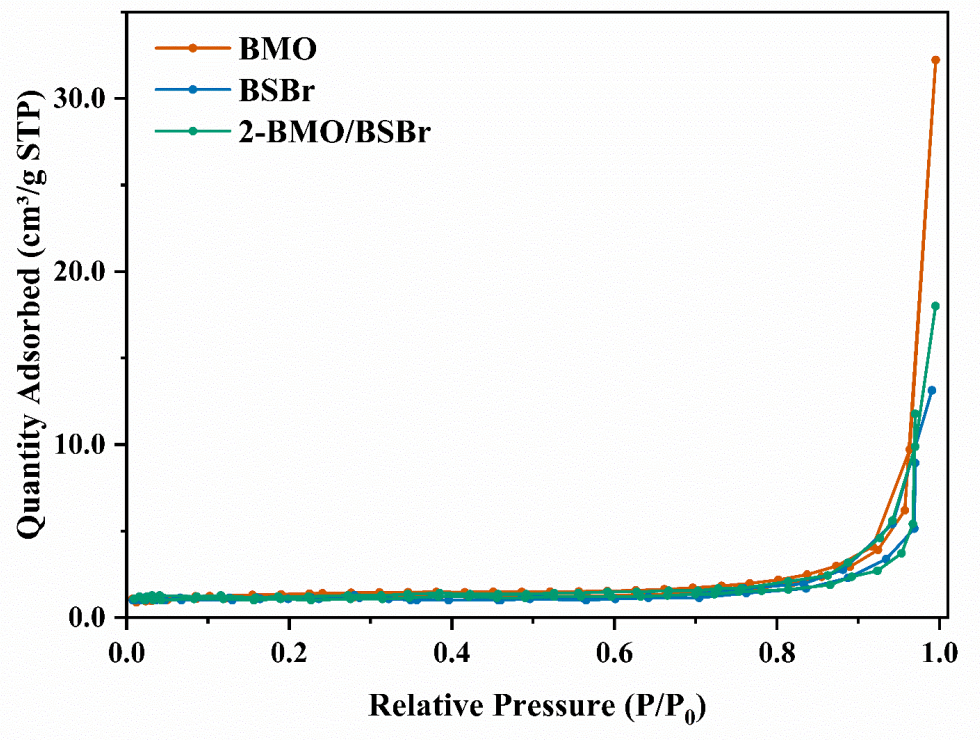
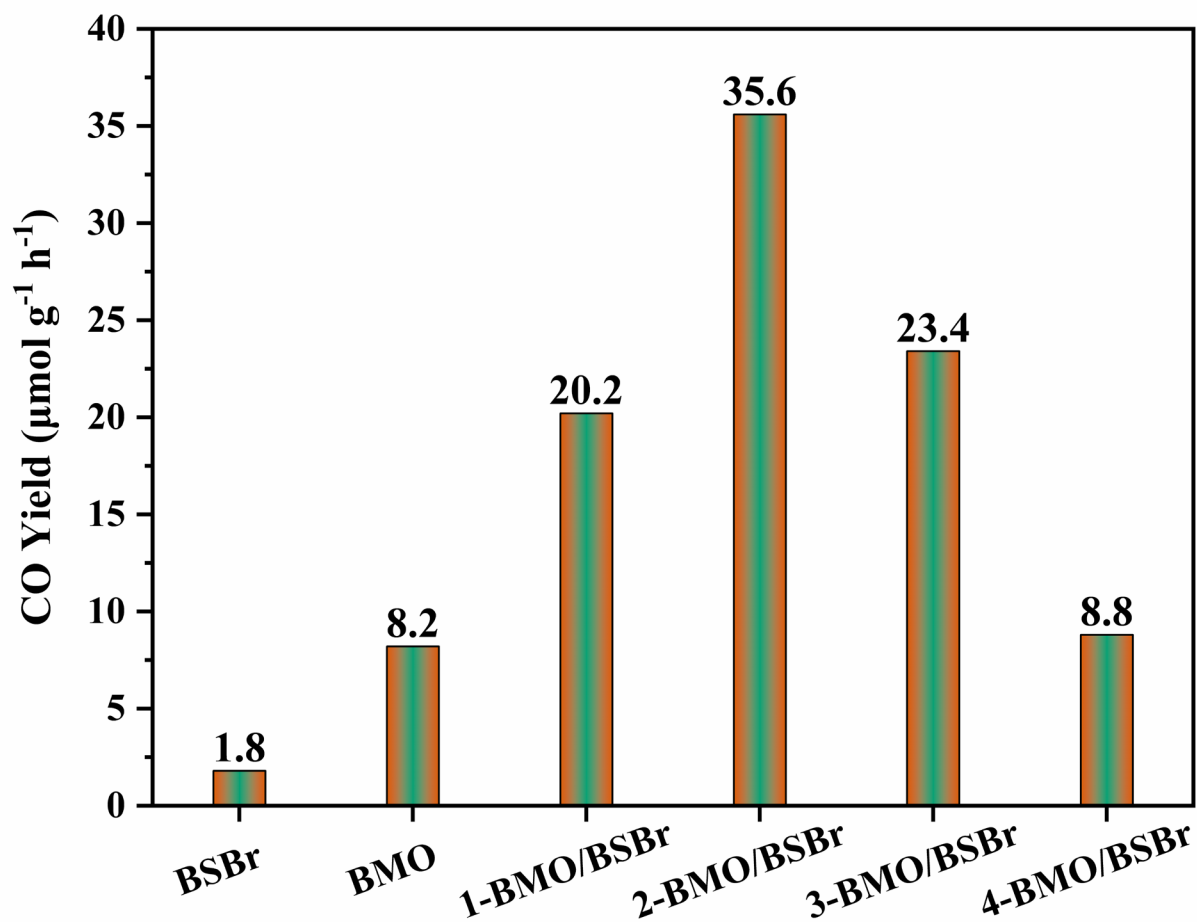


Figure S5. EDS spectra of 2-BMO/BSBr sample.



**Figure S6.** BET test of BMO, BSBr, and 2-BMO/BSBr samples.



**Figure S7.** Photocatalytic CO evolution for the prepared samples under full light spectrum.

After 5 h of full solar light irradiation, the CO production rates of the BMO and BSBBr are only 8.2 and 1.8  $\mu\text{mol g}^{-1} \text{h}^{-1}$ , respectively. In contrast, BMO/BSBr composite catalysts show substantially higher CO evolution. Among them, 2-BMO/BSBr demonstrated an optimal CO production rate of 35.6  $\mu\text{mol g}^{-1} \text{h}^{-1}$ . This result concludes that there is no significant difference in CO evolution between full spectrum and visible light irradiation for this system.

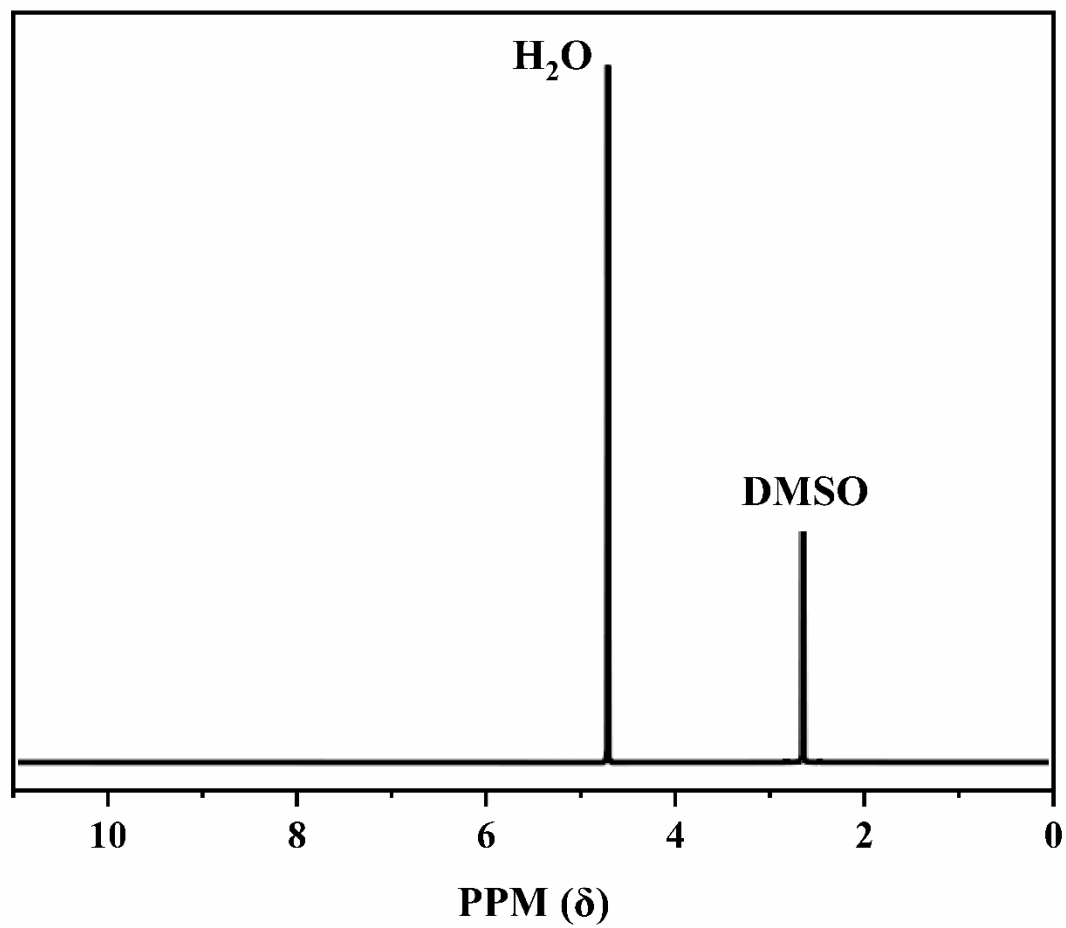


**Figure S8.** NMR spectrum of 2-BMO/BSBr sample after 5h irradiation.

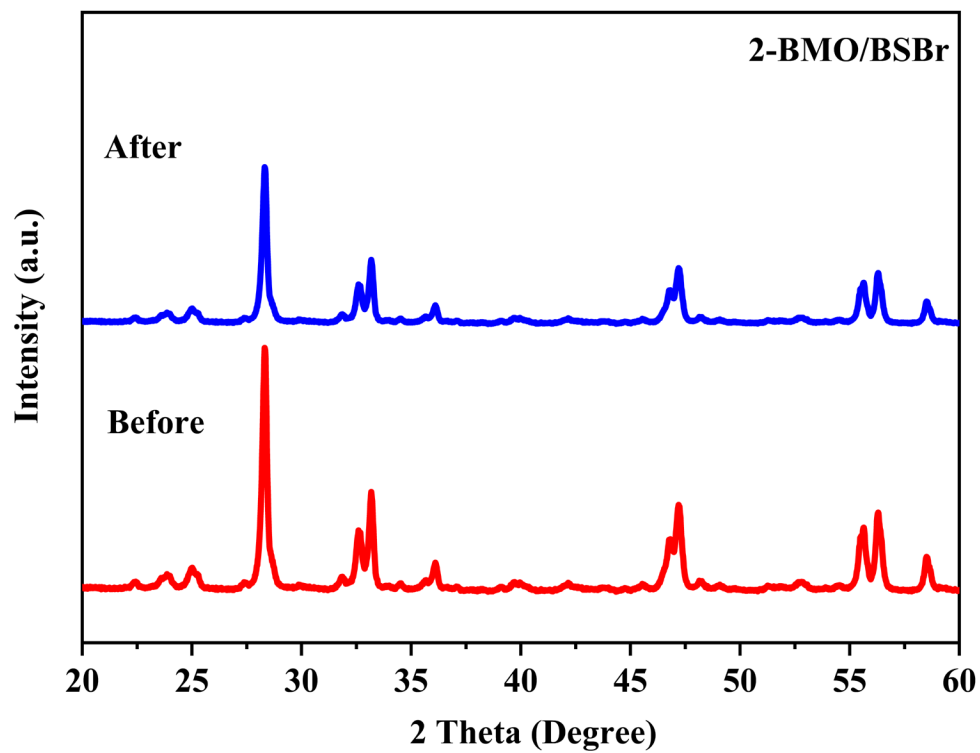


**Figure S9.** XRD patterns of 2-BMO/BSBr sample before and after cycle test.

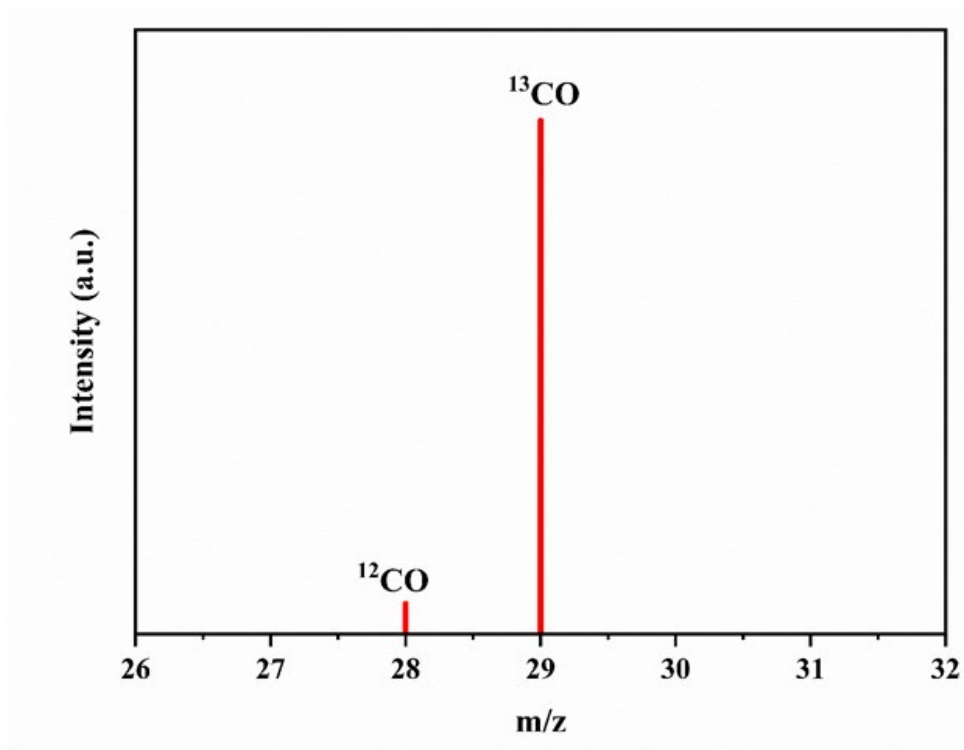


**Figure S10.** Mass spectra of  $^{13}\text{CO}$  over 2-BMO/BSBr in the photocatalytic reduction of  $^{13}\text{CO}_2$ .

**Table S1.** The recent CO<sub>2</sub> photoreduction performance of Bi-based materials without the addition of co-catalyst and sacrificial agent.

| Catalyst   | Light source    | System                             | The yield of production<br>( $\mu\text{mol g}^{-1} \text{h}^{-1}$ ) | Ref       |
|--|-----------------|------------------------------------|---|-----------|
| Bi <sub>2</sub> MoO <sub>6</sub> /Bi <sub>19</sub> S <sub>27</sub> Br <sub>3</sub> | 300W xenon lamp | CO <sub>2</sub> + H <sub>2</sub> O | 34.4  | This work |
| In <sub>2</sub> O <sub>3</sub> /Bi <sub>2</sub> MoO <sub>6</sub>                   | 300W xenon lamp | CO <sub>2</sub> + H <sub>2</sub> O | CO: 12.5<br>CH <sub>4</sub> : 4.02                                  | 1         |
| Bi <sub>2</sub> MoO <sub>6-x</sub> /MoS <sub>2</sub>                               | 300W xenon lamp | CO <sub>2</sub> + H <sub>2</sub> O | CO: 29.01   | 2         |
| Bi <sub>2</sub> MoO <sub>6</sub> @ZnIn <sub>2</sub> S <sub>4</sub>                 | 300W xenon lamp | CO <sub>2</sub> + H <sub>2</sub> O | CO: 23.11<br>CH <sub>4</sub> : 2.26                                 | 3         |
| Bi <sub>2</sub> MoO <sub>6</sub> @COF  | 300W xenon lamp | CO <sub>2</sub> + H <sub>2</sub> O | CO: 12.71<br>CH <sub>4</sub> : 5.5                                  | 4         |
| ZrO <sub>2</sub> /Bi <sub>19</sub> S <sub>27</sub> Br <sub>3</sub>                 | 300W xenon lamp | CO <sub>2</sub> + H <sub>2</sub> O | CO: 10.46<br>CH <sub>4</sub> : 18.04                                | 5         |
| Bi <sub>19</sub> S <sub>27</sub> Br <sub>3</sub> /g-C <sub>3</sub> N <sub>4</sub>  | 300W xenon lamp | CO <sub>2</sub> + H <sub>2</sub> O | CO: 12.87   | 6         |
| Bi <sub>19</sub> S <sub>27</sub> Br <sub>3</sub> / BiOBr                           | 300W xenon lamp | CO <sub>2</sub> + H <sub>2</sub> O | CO: 19.38   | 7         |

## Reference

1. F.-J. Zhang, Z.-C. Wang, Y.-H. Niu and J. Ma, *Solid State Sciences*, 2025, 108139.
2. H. Wei, F. Meng, H. Zhang, W. Yu, J. Li and S. Yao, *Journal of Materials Science & Technology*, 2024, **185**, 107-120.
3. J. He, J. Lin, Y. Zhang, Y. Hu, Q. Huang, G. Zhou, W. Li, J. Hu, N. Hu and Z. Yang, *Chemical Engineering Journal*, 2024, **480**, 148036.
4. Y. Wu, Y. Wang, M. Zhou, Y. Zhang, H. Li, Q. Liang, Z. Li and S. Xu, *Separation and Purification Technology*, 2025, 133081.
5. W. Ouyang, J. Zhao, J. Chen, Y. Wang, M. Xue, Y. Zhang, Z. Gong, J. Di, S. Yin and J. Xia, *Transactions of Tianjin University*, 2025, 1-15.
6. J. Zhao, M. Ji, H. Chen, Y.-X. Weng, J. Zhong, Y. Li, S. Wang, Z. Chen, J. Xia and H. Li, *Applied Catalysis B: Environment and Energy*, 2022, **307**, 121162.
7. J. Zhao, M. Xue, M. Ji, B. Wang, Y. Wang, Y. Li, Z. Chen, H. Li and J. Xia, *Chinese Journal of Catalysis*, 2022, **43**, 1324-1330.